Transport and magnetic anomalies below 70 K in a hydrogen-cycled Pd foil with a thermally grown oxide

Andrei Lipson,[1,2] Brent J. Heuser,[1,*] Carlos Castano,[1] George Miley,[1] Boris Lyakhov,[2] and Alexander Mitin[3]
[1]*University of Illinois, Department of Nuclear, Plasma, and Radiological Engineering, Urbana, Illinois, 61801 USA*
[2]*Institute of Physical Chemistry, Russian Academy of Sciences, Moscow, 119915 Russia*
[3]*P. L. Kapitza Institute for Physical Problems, Russian Academy of Sciences, Moscow, 119334 Russia*
(Received 27 May 2005; published 13 December 2005)

Electron transport and magnetic properties have been studied in a deformed 12.5-μm-thick Pd foil with a thermally-grown oxide and a low residual concentration of hydrogen. This foil was deformed by cycling across the Pd hydride miscibility gap and the residual hydrogen was trapped at dislocation cores. Anomalies of both resistance and magnetic susceptibility have been observed below 70 K, indicating the appearance of excess conductivity and a diamagnetic response that we interpret in terms of filamentary superconductivity. These anomalies are attributed to a condensed hydrogen-rich phase at dislocation cores near the Pd-Pd oxide interface.

DOI: 10.1103/PhysRevB.72.212507 PACS number(s): 74.10.+v, 72.15.−v, 61.72.Yx, 75.20.En

Homogeneous bulk palladium is not superconducting, at least above 3 mK,[1] while bulk Pd hydride and deuteride are superconducting, exhibiting an inverse isotope effect with critical temperatures between 7 and 9 K near stoichiometric compositions.[2,3] The effect of approaching stoichiometric compositions is dramatic, with the critical temperature increasing from approximately 1 to 8 K as the composition increases from $PdH_{0.8}$ to $PdH_{1.0}$.[2] The origin of superconductivity in Pd hydride is thought to be based on strong electron coupling to the optical phonon modes, requiring a suppression of spin fluctuations in the Pd lattice and *sd* hybridization of the hydrogen and Pd electrons.[4] Recently, Ashcroft has proposed that group IVa hydrides may exhibit high-temperature superconductivity (HTSC).[5] The central thesis in Ashcroft's work is that these hydrides are in a form of "precompression" due to the high electron density within the unit cell and additional external pressure can induce a metallic phase. The electrons from both the hydrogen and the group IVa element could then, according to Ashcroft, participate in common overlapping bands, leading to HTSC.[5]

In this Brief Report we present evidence of such a hydrogen-rich metallic phase, not in a group IVa hydride, but along dislocations near the interface of Pd and Pd oxide. Dislocation defects are strong, abundant traps of interstitial hydrogen and deuterium in deformed Pd. A high dislocation density, in excess of 2×10^{11} cm^{-2}, can be created in Pd by cycling across the hydride miscibility gap.[6] At low residual concentration, $\langle x\rangle\sim10^{-4}$ [H]/[Pd], hydrogen is strongly trapped (binding energy $\varepsilon_H\sim0.7$ eV/H atom), within approximately one Burgers vector (2.75 Å) of the dislocation core.[7] The local concentration at the dislocation core under these conditions is estimated at $\sim1-2$ [H]/[Pd].[8] The local pressure at a dislocation core is estimated to be comparable to the local bulk modulus (>100 GPa for Pd) (Ref. 9) and the conditions for hydrogen precompression are fulfilled.

Recently, a diamagnetic susceptibility contribution has been observed in hydride-cycled bulk Pd with $\langle x\rangle\sim10^{-4}$ [H]/[Pd].[8] Because of the low volume fraction and relatively uniform dislocation substructure of cycled Pd,[10] the diamagnetic response was not observed directly, but only after subtraction of the host Pd paramagnetic susceptibility. The volume fraction has been increased by cycling a thin Pd foil with a thermally-grown oxide layer. The oxide layer further constrained the Pd lattice during hydride cycling and prevented dislocation annihilation at the free surface. Both effects acted to increase the density of dislocation loops near the Pd-oxide interface, similar to the dispersive effect of internal precipitates.[11] We believe the dislocation enhancement promotes conditions favorable for a filamentary superconducting state not present in the cycled bulk Pd.[8]

The cold rolled Pd foil, supplied by Nilaco Co. of Japan, was 12.5-μm thick with purity of 99.95%. The concentration of ferromagnetic impurities (primarily Fe) did not exceed 10 ppm based on trace element analysis performed by the supplier. A 20 nm oxide layer was grown by heating the foil in an oxygen-propane flame at 1200 °C for ~6 s. Auger electron spectroscopy analysis showed that the oxygen content in the oxide layer below 1% at a depth 20 nm. The electrical resistivity and magnetic susceptibility characterization of the sample (~2 cm^2 area, 30 mg) prior to hydrogen cycling constitutes the background measurement and is referred to as Pd/PdO below. The sample was then cathodically loaded with hydrogen to $PdH_{0.7}$ at a current density of 5.0 mA/cm^2 in a 1 M Li_2SO_4/H_2O (99.99% pure) electrolyte. Hydrogen was removed from the sample by reversing the current, resulting in one hydrogen loading-unloading cycle. The sample used here was cycled five times. This procedure is known to produce a relatively uniform dislocation substructure as incoherent phase boundaries pass through the sample.[6,10,12] This substructure will be superimposed on the heterogeneous cellular substructure from cold rolling. The sample was finally annealed at 300 °C in vacuum of 10^{-7} Torr for 2 h to remove all but the strongest bound hydrogen. The electrical resistance and magnetic susceptibility characterization of the post-cycle annealed sample constitutes the foreground measurement and is referred to as $Pd/PdO:H_x$ below. The residual hydrogen concentration $\langle x\rangle$ was determined by thermal desorption analysis using a procedure described elsewhere[8] after the foreground resistance and magnetic susceptibility measurements. Current-voltage

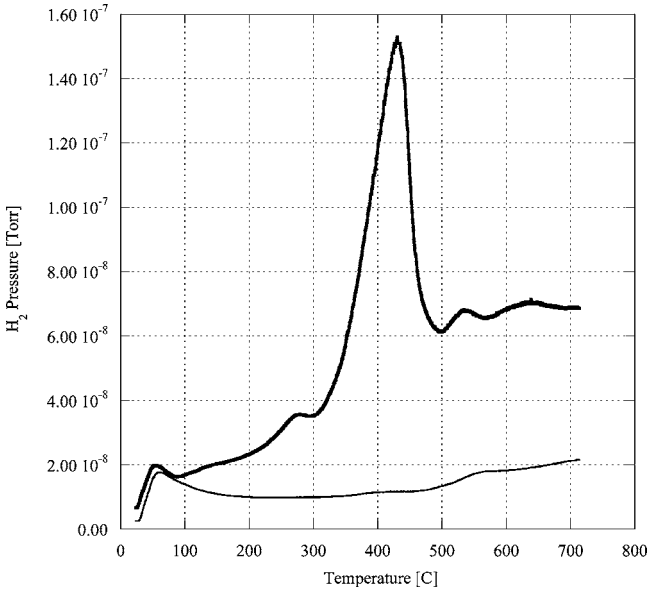

FIG. 1. Thermal desorption measurements of $Pd/PdO:H_x$ (thick solid line) and Pd/PdO (thin solid line).

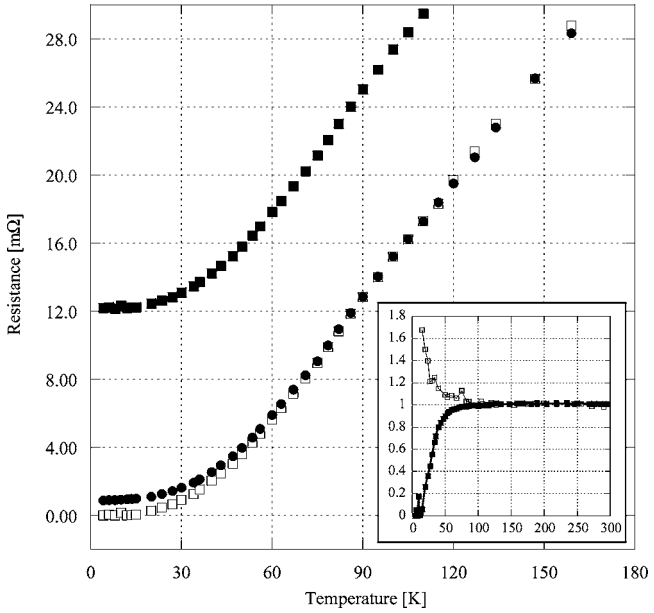

FIG. 2. Resistance versus temperature $R(T)$ for $Pd/PdO:H_x$ (solid boxes), Pd/PdO (solid circles), and $R(Pd/PdO:H_x) - 12.20\ m\Omega$ (open boxes, see text). The inset shows the ratios of resistance $[R(Pd/PdO:H_x) - 12.20\ m\Omega]/R(Pd/PdO)$ (solid boxes) and temperature coefficient of resistance $dR/dT(Pd/PdO:H_x)/dR/dT(Pd/PdO)$ (open boxes) versus temperature.

characteristics were measured with the standard four probe technique over a range of 4.2–295 K. The voltage was measured with a Keithley 182 digital voltmeter by passing rectangular current pulses of 1–10 s through the sample with fixed amplitude that varied over a range of 1 μA–10 mA. The current pulses were supplied by a Keithley 220 programmable source that excluded thermo-power contributions. Magnetic property measurements were performed with 1-T-SQUID Quantum Design MPMS-3 using both dc-magnetization and ac-susceptibility modes. Samples were mounted inside a gelatin capsule with the applied magnetic field both parallel ($H_\parallel$) and perpendicular ($H_\perp$) to the foil surface, the latter of which was measured with a sandwich of six pieces (resulting in an effective sample thickness of 75 μm) to increase the total volume of material.

Thermal desorption analysis (TDA) measurements of the $Pd/PdO:H_x$ and Pd/PdO samples are shown in Fig. 1. A sharp primary release peak near 430 °C superimposed on a much broader peak is evident in the $Pd/PdO:H_x$ measurement. The binding energies corresponding to the sharp and broad peaks are estimated as $\varepsilon_H = 0.65 \pm 0.10$ eV and $\varepsilon_H = 0.16 \pm 0.05$ eV, respectively, using the Garlick-Gibson model.[13] The higher energy is consistent with the result of Kirchheim for hydrogen trapping at dislocation core sites in cycled Pd.[7] The lower energy is consistent with much weaker hydrogen trapping interaction, possibly at dislocations within the underlying cellular dislocation substructure of the cold rolled foil Pd (Ref. 11) and at oxygen vacancies in the PdO. The concentration of hydrogen corresponding to the primary release peak is estimated as $\langle x \rangle = 6.0 \times 10^{-4}$ [H]/[Pd] based on calibration of the TDA system with TiH powder.[8] This is the concentration averaged over the entire volume of the sample. The local concentration within one Burgers vector (2.75 Å) of the dislocation core will be much higher and is estimated at $\langle \tilde{x} \rangle \sim 1.8$ [H]/[Pd] using simple geometric arguments with an assumed dislocation density of 2×10^{11} cm^{-2}.[8] Both the high binding energy and local concentration imply significant band overlap of the Pd and H electron states compared to bulk Pd hydrides with $x \leqslant 1$.

The resistance versus temperature for both samples measured with a current of 0.1 mA is shown in Fig. 2. The resistance of the $Pd/PdO:H_x$ sample includes a temperature-independent defect component associated with cycle-induced dislocation formation (Matthiessen's rule) equal to 12.20 ± 0.15 mΩ. This value was obtained by overlapping the resistance curves for $Pd/PdO:H_x$ and Pd/PdO above 200 K, where the contribution of the temperature-independent fraction of the full resistance is negligible.[14] The third curve in Fig. 2 corresponds to the temperature-dependent component of $Pd/PdO:H_x$ after the subtraction of the 12.20 mΩ value and exhibits enhanced conductivity relative to Pd/PdO below 70 K. This enhanced conductivity is best seen in the ratio of resistances shown in the Fig. 2 inset. The ratio of temperature coefficients of resistance (the normalized derivative) versus temperature are also shown in the inset of Fig. 2. The larger coefficient for the $Pd/PdO:H_x$ sample is an indication of a more metal-like behavior. Both the reduced resistance and enhanced temperature coefficient are attributed to condensation of hydrogen at dislocation cores into a metal-like phase.

The enhanced electron transport properties of the $Pd/PdO:H_x$ sample are supported by the $V(I)$ characteristics shown in Fig. 3. The normalized voltage ($Pd/PdO:H_x$ over Pd/PdO) is plotted versus dc current over the temperature range $4.2 < T < 203$ K. The nonlinear behavior at low current (<0.01 mA) and low temperature ($\leqslant 50$ K) indicate enhanced transport properties consistent with uncorrelated supercurrents[15] that break down at high current and high

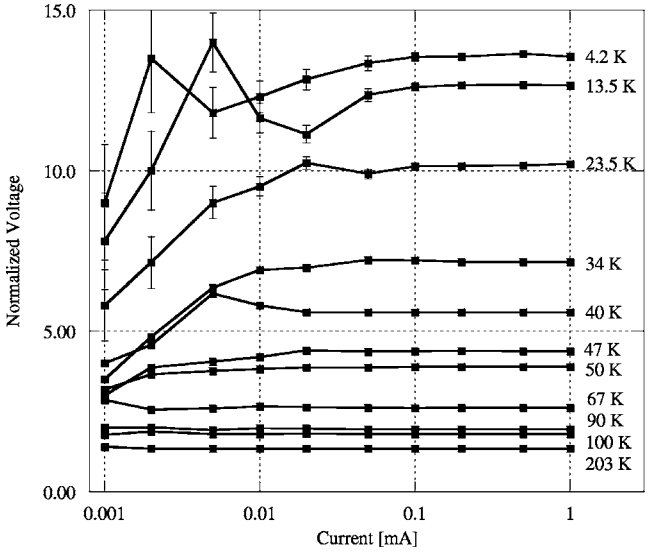

FIG. 3. Normalized voltage versus dc current characteristics $V(I)$ for the temperatures as labeled. The normalized voltage is the ratio of $V(\mathrm{Pd/PdO:H}_x)$ to $V(\mathrm{Pd/PdO})$. Nonlinear behavior is observed below 0.01 mA for temperatures below 67 K.

temperature ($T > 67$ K). Note that the observed nonlinearity is not a result of statistical fluctuations in the $V(I)$ measurement. We believe the nonlinear behavior is associated with the suppression of weak superconductivity along a network of condensed hydrogen at dislocation cores analogous to a Josephson medium. Similar filamentary superconductivity has been previously observed in high-T_c superconductors.[16,17]

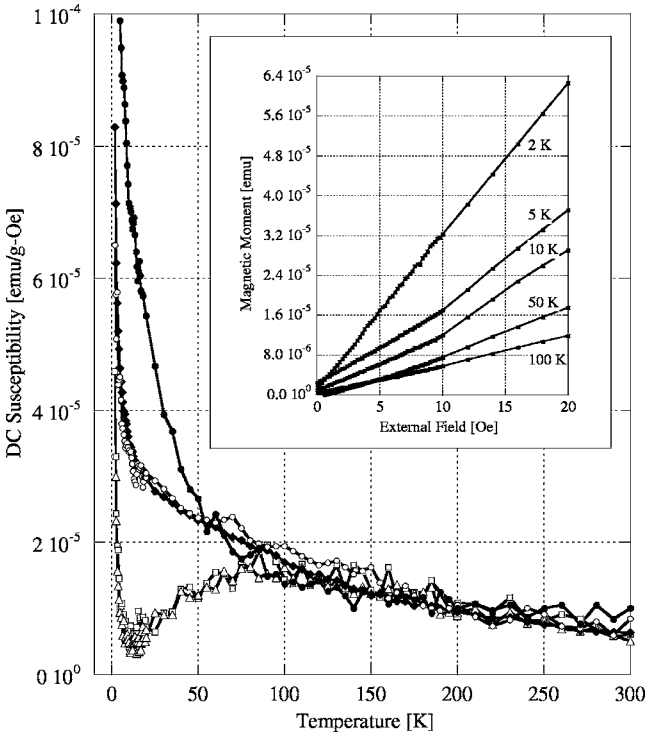

FIG. 4. dc susceptibility versus temperature for $\mathrm{Pd/PdO:H}_x$ under ZFC at 1.0 Oe (open boxes), 1.5 Oe (open triangles), and 5.0 Oe (solid diamonds), under FC conditions at 1.0 Oe (solid circles), and for Pd/PdO under ZFC at 1.0 Oe (open circles). The inset shows low-field magnetization versus field at the temperatures as labeled.

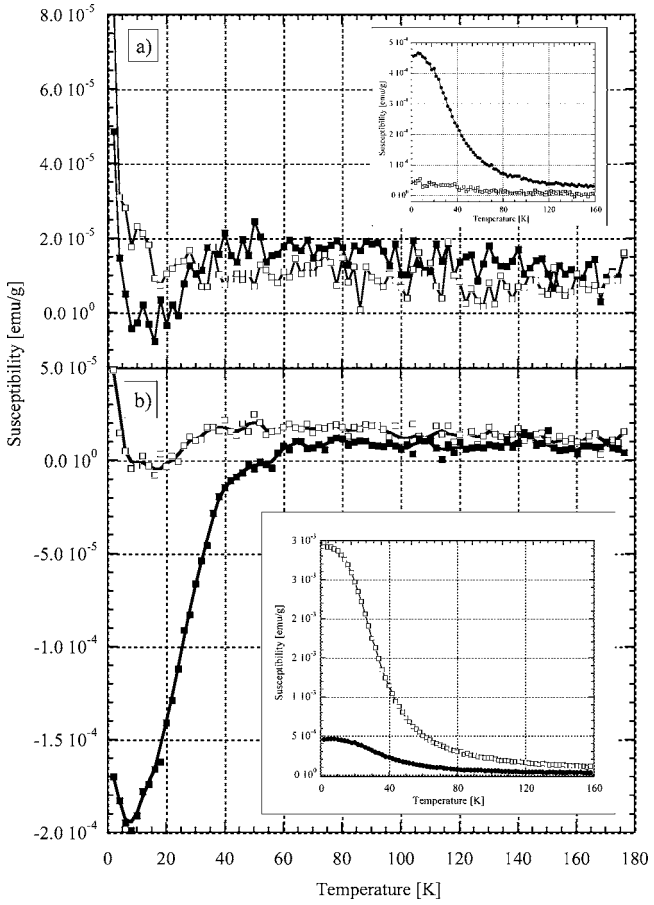

FIG. 5. (a) Real ac susceptibility versus temperature for parallel orientation of $\mathrm{Pd/PdO:H}_x$ (solid boxes) and Pd/PdO (open boxes) with parallel applied field; (b) real ac susceptibility versus temperature for $\mathrm{Pd/PdO:H}_x$ in perpendicular (solid boxes) and parallel (open boxes) orientation. Measurements were performed with $H=0$, a driving amplitude of 1 Oe, and a frequency of 992 Hz. Insets show corresponding imaginary ac component with the same symbol identifications.

dc susceptibility measurements of both samples are shown in Fig. 4. The zero-field-cooled (ZFC) measurement of $\mathrm{Pd/PdO:H}_x$ at 1.0 and 1.5 Oe exhibits a transition below $\sim$70 K, manifested as a reduction of the dc susceptibility (the sharp *increase* in susceptibility below 5 K is due to ferromagnetic impurities[18] and nonstoichiometric oxygen in the PdO layer). This transition is not present at a larger applied field, in the field-cooled (FC) condition, nor in the Pd/PdO zero-field-cooled background measurement at 1.0 Oe. The transition is attributed to a diamagnetic contribution to the paramagnetic response of Pd resulting from condensation of the trapped residual hydrogen. Additional proof is found in the magnetization versus applied field shown in Fig. 4, inset. The 5, 10, and 50 K measurements of the $\mathrm{Pd/PdO:H}_x$ sample exhibit an inflection between 5 and 7.5 Oe that are not observed in paramagnetic materials. The change in slope is absent below 5 and above 50 K consistent with the para-

magnetic response of Pd containing ferromagnetic impurities.

ac susceptibility measurements were performed to provide a more sensitive verification of the diamagnetic contribution. Real and imaginary ac susceptibility components for the two samples are shown in Fig. 5. The real component of the Pd/PdO:H_x is weakly diamagnetic below ~40 K when the sample is oriented parallel to the applied ac field, while that of the Pd/PdO sample is weakly paramagnetic [Fig. 5(a)]. The imaginary components differ as well, with the Pd/PdO:H_x sample exhibiting a peak that is absent in the Pd/PdO sample [Fig. 5(a) inset]. The onset of the weak diamagnetic behavior and the peak in the imaginary susceptibility coincide with a magnetic phase transformation. The diamagnetic response is enhanced by a factor of 30 when the Pd/PdO:H_x sample is perpendicular to the applied ac field [Fig. 5(b)].

One possible origin of the diamagnetic response from Pd/PdO:H_x in Fig. 5 is magnetic field expulsion due to the skin effect under an applied ac field. The skin depth is proportional to $\delta(T) \sim [\sigma(T)]^{-1/2}$, where $\sigma(T)$ is the conductivity corresponding to the resistance of Pd/PdO:H_x in Fig. 2. The estimated skin depth ($\delta \sim 2.9-3.6$ mm over the temperature range 5 to 60 K) is much greater than the effective sample thickness of 75 μm. Flux expulsion from the foil can account for at most 5% of the observed diamagnetic response in the perpendicular-field condition. We therefore assign the diamagnetic transition observed in the ac susceptibility measurements to the presence of a minute fraction of a superconducting phase in the Pd/PdO:H_x matrix. Accordingly, the behavior of the low-temperature ac susceptibility in the parallel- and perpendicular-field conditions is in agreement with two-dimensional type-II superconductivity when the coherence length is larger than the width of the superconducting layer.[19]

The emergent superconducting network is consistent with McMillan's estimate of the critical temperature[20]

$$T_c = (\langle \hbar\omega \rangle / 1.2 k_B) \times \exp\left[- \frac{1.04(1+\lambda)}{\lambda - \mu^*(1+0.62\lambda)} \right], \quad (1)$$

where $\langle \hbar\omega \rangle \sim 58-105$ meV is the characteristic average of phonon energy in the condensed phase, $\lambda = \lambda(\mathrm{Pd}) + \lambda(\mathrm{H})$ is the electron-phonon coupling constant from the Pd and hydrogen subsystems, and $\mu^* \sim 0.1$ is the Coulomb pseudopotential that accounts for the repulsive effect between electrons. The values for $\langle \hbar\omega \rangle$ and μ^* used here have been discussed previously.[8] The electron-phonon coupling constant is estimated as $\lambda = 0.89$ for $\langle \tilde{x} \rangle = 1.8$ based on a linear extrapolation of coherent inelastic neutron diffraction data from Rowe *et al.*[8,21] The estimated $T_c \sim 40-70$ K agrees with the onset of both excess conductivity and diamagnetism observed in the Pd/PdO:H_x sample.

In summary, we have observed anomalies in the electron transport and magnetic properties in a deformed Pd foil with a thermally-grown oxide layer and a small residual hydrogen concentration trapped at dislocations. The anomalies are consistent with a filamentary superconducting network that we attribute to the condensation of the trapped hydrogen into a metallic-like phase within the dislocation core. Dislocation pileup at the Pd-Pd oxide interface is thought to promote the filamentary nature of the network. This phase represents a hydrogen dominant metallic alloy, where both hydrogen and palladium atoms may participate in common overlapping bands.[5] Finally, we note that the presence of nonstoichiometric oxygen near the Pd-oxide layer interface may enhance electron-phonon coupling and therefore increase the critical temperature, similar to the cuprates.[22]

This work was partially supported by the NSF under Grant No. DMR-9982520. The magnetic property measurements were performed at the Frederick Seitz Material Research Laboratory at UIUC supported by the U.S. Department of Energy under Grant No. DEFG02-91-ER45439. The authors would like to thank Dr. A. Bezryadin (UIUC) and Dr. R. Prozorov (Univ. South Carolina) for useful comments.

*Author to whom correspondence should be addressed

[1] B. Strizker and H. Wuhl, in *Hydrogen in Metals II. Topics in Applied Physics*, edited by G. Alefeld and J. Völkl (Springer Verlag, Berlin, 1978), Vol. 29.
[2] J. E. Schriber and C. J. M. Northrup, Jr., Phys. Rev. B **10**, 3818 (1974).
[3] B. Stritzker, Phys. Rev. Lett. **42**, 1769 (1979).
[4] L. Schlapbach, I. Anderson, and J. P. Burger, in *Material Science and Technology*, edited by K. H. Jurgen Buschow (Weinheim, New York, 1994), Vol. 3B, Pt. II, p. 287.
[5] N. W. Ashcroft, Phys. Rev. Lett. **92**, 187002 (2004).
[6] B. J. Heuser and J. S. King, J. Alloys Compd. **261**, 225 (1997).
[7] R. Kirchheim, Acta Metall. **29**, 845 (1981).
[8] A. G. Lipson *et al.*, Phys. Lett. A **339**, 414 (2005).
[9] J. P. Hirth and J. Lothe, *Theory of Dislocations*, 2nd ed. (Krieger, Malabar, FL, 1982).
[10] B. J. Heuser and J. S. King, Metall. Mater. Trans. A **29**, 1594 (1998).
[11] D. Wang *et al.*, J. Alloys Compd. **348**, 119 (2003).
[12] M. Maxelon *et al.*, Acta Mater. **49**, 2625 (2001).
[13] G. F. J. Garlick and A. F. Gibson, Proc. Phys. Soc. London **60**, 574 (1948).
[14] N. E. Alekseevskii *et al.*, Physica B **163**, 659 (1990).
[15] A. A. Abrikosov, Phys. Rev. B **64**, 104521 (2001).
[16] P. M. Grant *et al.*, Phys. Rev. Lett. **58**, 2482 (1987).
[17] C. Panagopoulos, M. Majoros, and A. P. Petrović, Phys. Rev. B **69**, 144508 (2004).
[18] H. C. Jamieson and F. D. Manchester, J. Phys. F: Met. Phys. **2**, 323 (1972).
[19] M. Tinkham, *Introduction to Superconductivity*, 2nd ed. (McGraw-Hill, New York, 1996.
[20] W. L. McMillan, Phys. Rev. **167**, 331 (1968).
[21] J. M. Rowe *et al.*, Phys. Rev. Lett. **57**, 2955 (1986).
[22] L. Pintschovius *et al.*, Phys. Rev. B **69**, 214506 (2004).